

PACS numbers: 87.64.K–; 78.35.+c; 78.47.Fg; 82.35.Pg
DOI: 10.1070/QE2010v040n12ABEH014471

Low-frequency four-wave mixing spectroscopy of biomolecules in aqueous solutions

A.F. Bunkin, S.M. Pershin

Abstract. **Four-wave mixing (FWM) spectroscopy is used to detect the rotational resonances of H_2O and H_2O_2 molecules in DNA and denatured DNA aqueous solutions in the range ± 10 cm^{-1} with a spectral resolution of 3 GHz. It is found that the resonance contribution of the rotational transitions of these molecules increases significantly in solutions rather than in distilled water. This fact is interpreted as a manifestation of specific properties of a hydration layer at DNA – water and denatured DNA – water interfaces. Analysis of the FWM spectra shows that the concentration of H_2O_2 molecules in the hydration layer of the DNA solution increases by a factor of 3 after denaturation. The FWM spectra of aqueous solutions of α-chymotrypsin protein are obtained in the range ± 7 cm^{-1} at the protein concentrations between 0 and 20 mg cm^{-3}. It is found that the hypersound velocity in the protein aqueous solution, measured by the shift of Brillouin components in the scattering spectrum, obeys a cubic dependence on the protein concentration and reaches a value of about 3000 m s^{-1} at 20 mg cm^{-3}.**

Keywords: *four-wave mixing spectroscopy, DNA, hydration layer.*

1. Introduction

It is well known that water plays a key role in the behaviour of protein molecules and deoxyribonucleic acid (DNA) under native conditions. One of the main goals of this paper is to study the interaction of a biopolymer surface with water, which is significant for understanding the mechanisms of protein folding [1 – 3], fluid flowing through capillaries and cellular membrane permeability [4], stability of biological structures in aqueous solutions [5]. It has been established [6 – 9] that the properties of water surrounding biopolymers differ considerably from those of bulk water without biomolecules. However, the reason of this difference is still unclear. Simulations of the molecular dynamics have shown that there exist rather rigid water structures around some proteins [6, 7] and carbohydrates [8] in the contact (hydration) layer. For example, the hydration layer prevents erythrocytes from approaching each other in an aqueous suspension as well as interferes with reaching the ultimate concentration of the erythrocytes which is determined by their geometrical dimensions. In this case, the hydration layer thickness can be several microns with the human red blood cell being ~ 7 μm in diameter [10]. Such structures were studied by different methods, including the microwave absorption spectroscopy [9]. However, serious problems arise here because of strong absorption of water in the far-IR spectral range, which necessitates measurements in thin liquid layers (typically between 25 and 450 μm) under conditions of uncontrolled local heating, i.e., under unnatural conditions.

Research on hydration layers of biomolecules and nanoparticles with the help of optical spectroscopy is mainly hampered by the fact that the hydration layer contains few molecules whose signal should be extracted against the background of the signal of water molecules residing outside the hydration layer. Therefore, the applied method should be nondestructive, rather sensitive (i.e., to have a high signal-to-noise ratio), and produce minimal perturbations (for example, heating). Such an approach should enable one to perform measurements in the region where the optical spectrum maximally depends on the intermolecular interaction. For water this region lies in the range from units to approximately 200 cm^{-1}, where intermolecular translational (~ 180 cm^{-1}) and transverse (~ 60 cm^{-1}) vibrations are located.

A promising approach to the solution of such problems is four-wave mixing (FWM) spectroscopy [11, 12], which employs two laser fields with the frequencies ω_1 and ω_2 in the visible spectral region, i.e., in the transparency window of the biological sample. In this case, the difference of these frequencies $(\omega_1 - \omega_2)$ is scanned in the low-frequency range. In our experiments the available spectral range was

$$-1200 \text{ cm}^{-1} < (\omega_1 - \omega_2)/2\pi c < 300 \text{ cm}^{-1},$$

where c is speed of light in vacuum. In this case, two laser beams with the frequencies ω_1 and ω_2 intersect in a liquid at an angle of $\sim 170^\circ$. The physics of four-photon interaction in this region of frequency detunings ($\omega_1 - \omega_2 = 0 - 36$ THz) allows a wide set of phase-matching angles; therefore, we used the given intersection angle of the beams to ensure the maximal length of the region of their intersection under spatial separation conditions. The optical path length of laser pulses was selected so that the pulses met inside the sample. The parameter to be measured is the intensity [at a frequency $\omega_s = \omega_1 - (\omega_1 - \omega_2)$] of signal radiation propagated through a polarisation analyser with

A.F. Bunkin, S.M. Pershin Wave Research Center, A.M. Prokhorov General Physics Institute, Russian Academy of Sciences, ul. Vavilova 38, 119991 Moscow, Russia; abunkin@kapella.gpi.ru, pershin@kapella.gpi.ru

Received 30 September 2010
Kvantovaya Elektronika **40** (12) 1098 – 1102 (2010)
Translated by I.A. Ulitkin

the wave polarisation $\boldsymbol{E}^{(2)}$ whose nonlinear polarisability is given by [11, 12]

$$\boldsymbol{P}_i^{(3)} = 6\chi_{ijkl}^{(3)}(\omega_s;\omega_1;\omega_2;-\omega_1)\boldsymbol{E}_j^{(1)}\boldsymbol{E}_k^{(2)}\boldsymbol{E}_l^{(1)*}. \quad (1)$$

Here, $\chi^{(3)}$ is the cubic susceptibility of the medium, proportional to the correlation function of optical anisotropy fluctuations; $\boldsymbol{E}^{(1)}$ and $\boldsymbol{E}^{(2)}$ are the amplitudes of the interacting fields; and $I_s \propto |\chi^{(3)}|^2 I_1^2 I_2$ is the four-wave mixing signal intensity. In this approach, alignment of the frequency difference $\omega_1 - \omega_2$ to a frequency of some vibrational or rotational molecular resonance on this transition in the medium under study results in the emergence of an ensemble of coherent states described by collective quantum-mechanical variables.

Using the FWM technique, we observed earlier [13–16] the rotational Raman lines of H_2O molecules in distilled water and aqueous solutions, as well as well-resolved rotational lines of H_2O, H_2O_2, and OH molecules in FWM spectra of distilled water. The spectral resolution of the spectrometer (~ 0.12 cm^{-1}, i.e., ~ 3.6 GHz) made it possible to attribute the rotational lines of H_2O molecules to transitions of ortho- and para-isomers. Here, ortho-isomers are the H_2O molecules in which the spins of protons are parallel and the total nuclear spin is equal to unity, and para-isomers are the H_2O molecules in which the proton spins are directed oppositely and the total spin is zero. The appearance of rotational spectra of H_2O is interpreted as the result of free rotation of water molecules in the low-density layers near the nanoparticles of hydrophobic impurities that exist in any kind of distilled water [17, 18]. Recently, this conclusion about the presence of free H_2O molecules in liquid water has been confirmed in another experiment using small-angle X-ray spectroscopy with the synchrotron of the fifth generation in Stanford (USA) [19].

In this paper, we will concentrate on studying FWM spectra of aqueous solutions of DNA and denatured DNA in the spectral range ± 10 cm^{-1}. In addition, we will analyse the FWM spectra of α-chymotrypsin protein at the different concentrations in aqueous solutions. We will show that the shift of Brillouin resonances of the aqueous protein solution depends on the protein concentration and monotonically increases with increasing concentration. This behaviour of the solution elasticity can be explained by a noticeable change in the properties of the interface layer between bulk water molecules and the protein.

2. Experimental

We performed the experiments using the setup described in detail in [20]. Two counterpropagating waves $\boldsymbol{E}^{(1)}$ and $\boldsymbol{E}^{(2)}$ with frequencies ω_1 and ω_2 propagated in a cell ($20 \times 30 \times 50$ mm) filled with aqueous solutions of biopolymers at room temperature. The cell input and output windows were made of fused quartz so that the depolarisation of transmitted laser radiation did not exceed 10^{-3}. The wave $\boldsymbol{E}^{(1)}$ (the second harmonic of a 532-nm single-longitudinal-mode Nd:YAG laser; the spectral width, less than 0.01 cm^{-1}) was circularly polarised with the intensity ~ 60 MW cm^{-2} inside the cell with a liquid. The wavelength tunable (500–545 nm) radiation $\boldsymbol{E}^{(2)}$ of the dye laser was linearly polarised and had the intensity of no more than 10 MW cm^{-2}. The laser pulse repetition rate was 1 Hz and the pulse duration was ~ 10 ns.

With such polarisations of interacting laser waves in the signal that is determined by nonlinearity (1), the nonresonant contribution from the electronic subsystem of the medium is absent [11, 12]. This circumstance is explained by the fact that when one of the pump waves is circularly polarised, the effective cubic susceptibility of centrosymmetric medium has the form [11, 12]

$$\chi^{(3)}(\omega_s;\omega_1;\omega_2;-\omega_1) = \chi_{1122}^{(3)}(\omega_s;\omega_1;\omega_2;-\omega_1) - \chi_{1212}^{(3)}(\omega_s;\omega_1;\omega_2;-\omega_1). \quad (2)$$

When Kleinman relations [12] are fulfilled for the components of the nonresonant (electronic) susceptibility tensor $\chi_{ijkl}^{(3)\mathrm{nr}}(\omega_s;\omega_1;\omega_2;-\omega_1)$, the nonresonant (nondispersive) pedestal in the FWM spectra vanishes because $\chi_{1122}^{(3)\mathrm{nr}}(\omega_s;\omega_1;\omega_2;-\omega_1) = \chi_{1212}^{(3)\mathrm{nr}}(\omega_s;\omega_1;\omega_2;-\omega_1)$. This is invalid, in the general case, for resonant tensor components $\chi_{ijkl}^{(3)\mathrm{r}}(\omega_s;\omega_1;\omega_2;\ -\omega_1)$ related to the molecular vibrations and rotations as well as fluctuations of the medium density and entropy.

Because the polarisation vectors of the coherent signal wave $\boldsymbol{E}_s$ generated at the frequency ω_s and of the wave $\boldsymbol{E}^{(2)}$ are noncollinear, while their propagation directions coincide, these waves can be separated from each other by a Glan prism. The width of the instrumental function of the spectrometer (~ 0.12 cm^{-1}) and the possible spectral measurement range ($-1200...300$ cm^{-1}) were determined by the parameters of the dye laser, which was pumped by the third harmonic of the Nd:YAG laser and provided computer-programmable tuning of the radiation wavelength $\boldsymbol{E}^{(2)}$. For each value of the wavelength ω_s, we performed averaging of the signal over 10–30 readings. Then, the frequency of the dye laser was tuned automatically with a step 0.119 cm^{-1}. The zero frequency was detuned with respect to Brillouin resonances, while further wavelength tuning was controlled by the modes of the Fabry–Perot interferometer with a base of 7 mm. The error in measuring the FWM signal amplitude was programmed and did not exceed 10 %. The accuracy in measuring the FWM signal amplitude was determined by the width of the instrumental function of the spectrometer; therefore, when fitting the envelopes with the tabulated data, we could observe a discrepancy with the measured contour within this quantity.

We performed measurements in twice-distilled Milli-Q (MQ) water, aqueous solutions of commercially available α-chymotrypsin protein (with a concentration up to 20 mg cm^{-3}), native DNA (15 mg cm^{-3}), denatured DNA (with the same concentration), and in a 1-% hydrogen peroxide solution (H_2O_2). The FWM signal appeared in the region (of length ~ 5 mm) of intersection of laser beams in the sample. No additional degassing of the liquids under study was performed. The DNA molecules were extracted using the procedure described in [21]. DNA was denaturated by heating the solution up to 90 °C followed by cooling to room temperature.

3. Results

Figure 1 shows the FWM spectra of H_2O_2 (with a concentration of 1 %) and DNA (15 mg cm^{-3}) aqueous solutions in the range from -1 to 5 cm^{-1}. The hydrogen peroxide solution was used as a reference sample with the known rotational spectrum of the H_2O_2 molecule. The

dashed arrows in Fig. 1 indicate the rotational resonances of the H_2O_2 molecule: $(2_{11} - 1_{01})$ (1.25 cm^{-1}), $(8_{27} - 9_{19})$ (1.47 cm^{-1}), $(7_{07} - 7_{17})$ (2.75 cm^{-1}), $(9_{09} - 9_{19})$ (3.06 cm^{-1}), $(10_{010} - 10_{110})$ (3.24 cm^{-1}), $(14_{014} - 14_{114})$ (4.12 cm^{-1}), $(16_{016} - 16_{116})$ (4.65 cm^{-1}); the thin arrow shows the ortho-isomer transition $(6_{16} - 5_{23})$ (0.74 cm^{-1}) of the H_2O molecule, respectively. It follows from this figure that the strongest rotational lines of H_2O and H_2O_2 molecules in DNA and H_2O_2 aqueous solutions coincide with the accuracy up to the width of the instrumental function of the spectrometer.

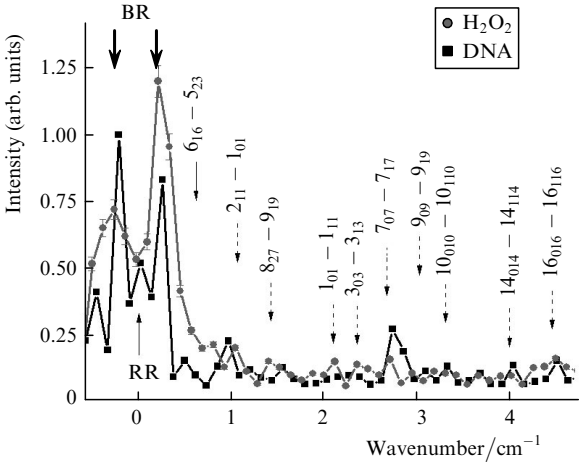

Figure 1. FWM spectra of laser radiation in aqueous solutions of hydrogen peroxide and DNA. Each experimental point is the result of accumulation over 30 laser shots with spectral step of ~ 0.12 cm^{-1}. Bold arrows show Brillouin resonances (BR) in the DNA aqueous solution. Dashed and thin (above) arrows indicate different rotational Raman lines of H_2O_2 and H_2O molecules, respectively, according to [22]; the thin arrow (below) shows the Rayleigh resonance (RR).

Figure 2 shows the FWM spectra of DNA (15 mg cm^{-3}) and MQ water in the range from 1 to -7 cm^{-1}, where the thick and thin arrows indicate Brillouin and Rayleigh resonances, respectively. For analysis convenience, the spectra are normalised to the amplitude of the Brillouin component. One can see from Fig. 2 that the contribution to the FWM signal from the rotational resonances of the H_2O and H_2O_2 molecules increases markedly in the DNA solution spectrum compared to the MQ water spectrum.

Figure 3 presents the experimental and calculated FWM spectra of the DNA (15 mg cm^{-3}) aqueous solution as well as experimental and calculated FWM spectra of the denatured DNA (with the same concentration) aqueous solution. To calculate the FWM spectra, we used standard expressions [12]:

$$\chi^{(3)} = \chi^{\mathrm{nr}} + \frac{\chi^{\mathrm{B}}}{-\mathrm{i} + (\Delta \pm \Omega_{\mathrm{B}})/\Gamma_{\mathrm{ap}}} + \frac{\chi^{\mathrm{R}}}{-\mathrm{i} + \Delta/\Gamma_{\mathrm{R}}}$$

$$+ \frac{\sum_n \chi_n^{\mathrm{rot}}}{-\mathrm{i} + (\Delta \pm \Omega_n)/\Gamma_{\mathrm{ap}}}, \quad I_{\mathrm{s}} \propto |\chi^{(3)}|^2 I_{\mathrm{I}}^2 I_2, \qquad (3)$$

where $2\Gamma_{\mathrm{ap}}$ is the spectral resolution of the FWM spectrometer (0.12 cm^{-1}); Γ_{R} is the half bandwidth of the Rayleigh wing spectrum (fitting parameter); χ_n^{rot} and Ω_n are the resonant nonlinear susceptibility and central frequency (in cm^{-1}) of the rotational resonances for

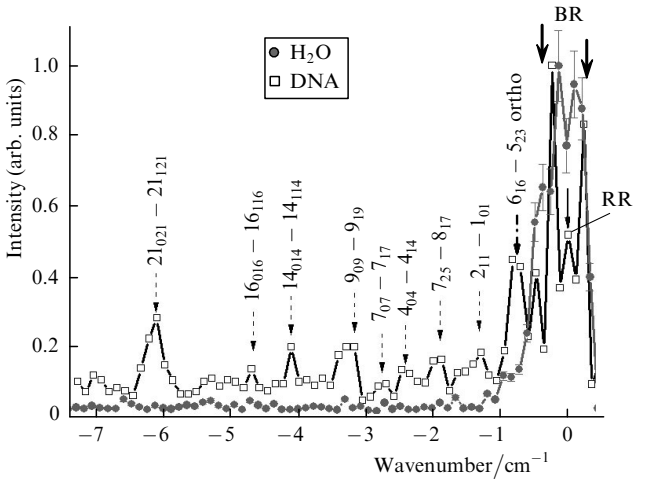

Figure 2. FWM spectra of the DNA aqueous solution and MQ water. Thick and thin arrows show Brillouin and Rayleigh resonances, respectively. Dashed arrows show different rotational Raman lines of H_2O_2 molecules; the dash-and-dot arrow shows the Raman $(6_{16} - 5_{23})$ (± 0.74 cm^{-1}) ortho-isomer line of the H_2O molecule.

H_2O_2 and H_2O molecules; Ω_{B} is the Brillouin resonant frequency for DNA and denatured DNA aqueous solutions, which was measured experimentally; $\Delta = (\omega_1 - \omega_2)/2\pi c$ is the frequency detuning (in cm^{-1}); χ^{B}, χ^{R} and χ^{nr} are nonlinear susceptibilities of Brillouin and Rayleigh resonances, as well as nonresonant nonlinear susceptibility of the solution, respectively. The spectroscopic data for H_2O_2 and H_2O molecules were taken from [22]. The relative concentration of H_2O_2 and H_2O molecules was used in calculations as a fitting parameter. The increase in the hydrogen peroxide concentration in the denatured DNA solution can be estimated by comparing the fitting parameters of DNA [curve (*2*), Fig. 3] and denatured DNA [curve (*4*)] FWM spectra. One can see from Fig. 3 that the calculated and experimental spectra agree well. Comparison of the spectroscopic parameters $\chi^{\mathrm{rot}}/\chi^{\mathrm{B}}$ in the $7_{25} - 8_{17}$ line (1.93 cm^{-1}) of H_2O_2 for the calculated FWM

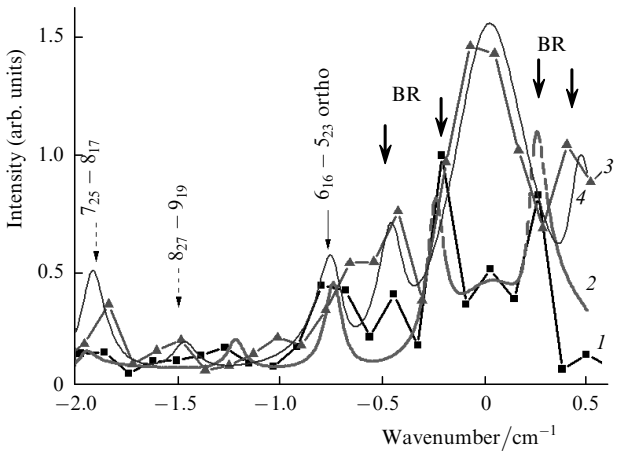

Figure 3. Experimental (*1*) and calculated (*2*) FWM spectra of the DNA aqueous solution (15 mg cm^{-3}) and experimental (*3*) and calculated (*4*) FWM spectra of denatured DNA aqueous solution with the same concentration. Dashed and thin arrows show rotational Raman lines of H_2O_2 and H_2O molecules; thick arrows show Brillouin resonances.

spectra of native DNA (0.4) and denaturated DNA (1.3) shows that the H_2O_2 concentration near the DNA molecules increases by a factor of ~ 3 during denaturation.

Figure 4a presents the FWM spectra of α-chymotrypsine protein aqueous solutions with the concentrations of 20 mg cm^{-3} and 10 mg cm^{-3} at room temperature. The positions of the Brillouin resonances are shown by bold arrows. One can see that the increase in the protein concentration is accompanied by the shift of the Brillouin resonances towards larger frequency detunings. We found experimentally that the shift of the Brillouin resonance frequency $\Delta\nu_B$ in the aqueous solution as a function of the relative protein concentration can be approximated by the dependence:

$$\Delta\nu_B = 0.25 + (5 \times 10^{16})P^3, \tag{4}$$

where P is the relative concentration of protein molecules in the aqueous solution. In Fig. 4, the solid curve is the calculation by (4) and points are the experiment.

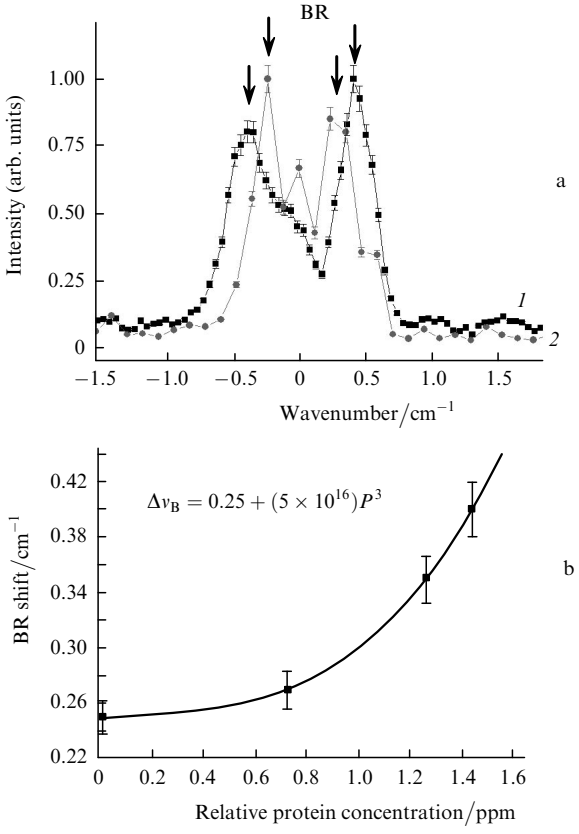

Figure 4. FWM spectra of the protein aqueous solutions with the concentrations of 20 (*1*) and 10 mg cm^{-3} (*2*) (a) and dependence of the Brillouin resonance shift in aqueous solutions on the protein concentrations in the range from 0 to 1.5 ppm (b).

The Brillouin resonant frequency shift is found from the expression [23]:

$$\Delta\nu_B = V_s(2n \sin\varphi/2)/c\lambda, \tag{5}$$

where n is the refractive index; λ is the wavelength of incident light; φ is the angle between incident and scattered waves; c is the speed of light; and V_s is the longitudinal speed of sound in the sample under study. For the parameters of MQ water at the room temperature, we have $n = 1.33$, $V_s = 1490$ m s^{-1} and $\lambda = 532$ nm and $\varphi = \pi$ for our experiments conditions. Then, according to (5), $\Delta\nu_B = 0.25$ cm^{-1}. It is known that the speed of sound V_s depends on the adiabatic compressibility K_s of the substance [23]:

$$(V_s)^2 = (\rho K_s)^{-1}, \tag{6}$$

where ρ is the mean mass density in the investigated volume. The noticeable increase in the speed of sound with increasing protein concentration in the aqueous solution (Fig. 4b) shows the corresponding decrease in the compressibility (increase in the elasticity) of water after introducing α-chymotrypsin protein molecules in the solution.

4. Discussion

Water is known to be a strongly associated liquid. Each molecule of water can form up to four hydrogen bonds with its neighbours. The average coordination number of hydrogen bonds at room temperature is equal to 3.5 [24]. Our experiments show that four-wave mixing spectra of water and aqueous solutions of biopolymers exhibit narrow resonances whose frequencies (within the accuracy of the instrumental function of the spectrometer) coincides with the frequencies of rotational transitions in the ground electronic and vibrational states of H_2O and H_2O_2 molecules. The increase in the resonance contribution of the rotational transitions of H_2O and H_2O_2 molecules when dissolving DNA molecules in water and denaturating DNA in an aqueous solution reflects the fact that at the water–biopolymer interface, there forms a layer of water, which has properties different from those of water in the bulk, and these properties experience further changes in the DNA denaturation [2, 17, 18].

It is also well known [25, 26] that hydration of biological molecules can lead to structurisation of water molecules of the hydration shell into assembles similar to the crystal lattice of hexagonal ice. This fact is qualitatively confirmed in our experiments by an increase in the Brillouin resonance shift and the corresponding increase in the solution compressibility with increasing protein concentration in an aqueous solution (Fig. 4). A similar increase in the Brillouin resonance shift was observed in DNA after denaturation (Fig. 3). Note that an increase in the erythrocyte concentration in an aqueous suspension [10] is accompanied by a decrease in the refractive index of water although the refractive index of an erythrocyte is larger than that of water. Zakharov et al. [10] interpreted this fact as the formation of a hydration layer with an ice-like structure because the refractive index of ice ($n_{ice} = 1.309$) is smaller than that of water (1.333).

The FWM spectra of the aqueous solutions of biopolymers exhibit an essential growth of the resonance contribution in the FWM signal from the rotational lines of the H_2O and H_2O_2 molecules compared to the corresponding lines in FWM spectrum of water (Fig. 2). This fact allows us to conclude that the molecules of biopolymers are capable of increasing significantly the effective concentration of free H_2O and H_2O_2 molecules in the hydration shell. Note that a similar effect has been recently observed in aqueous suspensions of single-wall carbon nanotubes [16] with a hydrophobic surface.

The cubic dependence of the shift of the Brillouin components on the protein concentration in an aqueous solution (Fig. 4b) shows indirectly that the hydration layer is formed in the bulk around the protein molecule as in the case of an erythrocyte [10]. Otherwise, if the layer were formed along the given direction or the plane, the concentration dependence of the shift would have a smaller refractive index. Possibly, it is this fact (the thickness of the hydration layer) that limits the solvability of proteins in water and determines the saturation concentration at this temperature. Obviously, the temperature rise will be accompanied by a 'melt' of the hydration layer, a decrease in its thickness, which will lead to an increase in the saturation concentration.

5. Conclusions

Thus, the four-wave mixing spectroscopy of proteins and DNA in water and aqueous solutions has shown that formation of the hydration shell of biomolecules is accompanied by a noticeable restructurisation of hydrogen bonds of water molecules. Some H_2O molecules in the vicinity of, obviously, hydrophilic residues of biomolecules form an ice-like structure, which manifests itself in an increase in the shift of the Brillouin components. In this case, other H_2O molecules upon rapture and formation of new hydrogen bonds rotate freely, obviously, in the vicinity of hydrophobic residues of biomolecules because an increase in the intensities of rotational lines of H_2O molecules is observed in the hydrophobic carbon nanotube suspension [16].

These conclusions agree with data on bulk water obtained by small-angle X-ray scattering spectroscopy [19], which simultaneously exhibits a characteristic peak of tetragonal clusters and free molecules. In addition, Pershin et al. [27] have recently observed the characteristic components of (3320 cm^{-1}) hexameric (ice-like) and tetrameric (3450 cm^{-1}) clusters in bulk water in the envelope of the OH band of stretching vibrations in the Raman spectra of the second harmonic radiation of an Nd:YAG laser. It is essential that when heating water to 99 °C the position of these frequencies was preserved, while the amplitudes varied out of phase: the contribution of hexameric clusters decreased, while that of small clusters increased (as in [19]).

Acknowledgements. This work was supported by the Russian Foundation for Basic Research (Grant Nos 09-02-01173, 08-02-00008, 10-02-90301-viet-a).

References

1. Garde S., Hammer G., Garcia A.E., Paulaitis M.E. Pratt L.R. *Phys. Rev. Lett.*, **77**, 4966 (1998).
2. Miller T.F., Vanden-Eijnden E., Chandler D. *Proc. Nat. Acad. Sci.*, **104**, 14559 (2007).
3. Liu P., Huang X.H., Zhou R.H., Berne B.J. *Nature (London)*, **437**, 159 (2005).
4. Zhu Y., Granick S. *Phys. Rev. Lett.*, **88**, 106102 (2002).
5. Levy Y., Onuchic J.N. *Proc. Nat. Acad. Sci.*, **101**, 3325 (2004).
6. Tarek M., Tobias D.J. *Phys. Rev. Lett.*, **89**, 275501 (2002).
7. Bizzarri A.R., Canistraro S. *J. Phys. Chem. B*, **106**, 6617 (2002).
8. Lee S.L., Debenedetti P.G., Errington J.R. *J. Chem. Phys.*, **122**, 204511 (2005).
9. Heugen U., Schwaab G., Brundermann E., Heyden M., Yu X., Leitner D.M., Havenith M. *Proc. Nat. Acad. Sci.*, **103**, 12301 (2006).
10. Zakharov S.D., Ivanov A.V., Wolf E.B., Danilov V.P., Murina T.M., Nguen K.T, Novikov E.G., Panasenko N.A., Perov S.N., Skopinov S.A., Timofeev Yu.P. *Kvantovaya Elektron.*, **33**, 149 (2003) [*Quantum Electron.*, **33**, 149 (2003)].
11. Shen Y.R. *The Principles of Nonlinear Optics* (New York: Willey, 1984).
12. Akhmanov S.A., Koroteev N.I. *Metody nelineinoi optiki v spektroskopii rasseyaniya sveta* (Methods of Nonlinear Optics in Light Scattering Spectroscopy) (Nauka, Moscow, 1981).
13. Bunkin A.F., Pershin S.M., Nurmatov A.A. *Usp. Fiz. Nauk*, **176**, 883 (2006) [*Phys. Usp.*, **49**, 855 (2006)].
14. Bunkin A.F., Pershin S.M., Nurmatov A.A. *Laser Phys. Lett.*, 3, 275 (2006).
15. Bunkin A.F., Pershin S.M. *J. Raman Spectr.*, **39**, 726 (2008).
16. Bunkin A.F., Pershin S.M. *Laser Phys. Lett.*, **4**, 656 (2007).
17. Miller T.F., Vanden-Eijnden E., Chandler D. *Proc. Nat. Acad. Sci.*, **104**, 14559 (2007).
18. Willard A.P., Chandler D. *J. Phys. Chem. B*, **112**, 6187 (2008).
19. www.pnas.org.cgi.doi.10.1073.pnas.0904743106.
20. Bunkin A.F., Nurmatov A.A. *Laser Phys.*, **13**, 328 (2003).
21. Bunkin A.F., Pershin S.M., Nurmatov A.A., Khusainova R.S., Potekhin S.A. *Kvantovaya Elektron.*, **37**, 941 (2007) [*Quantum Electron.*, **37**, 941 (2007)].
22. Rothman L., Jacquemart D., Barbe A., et al. *J. Quantum Spectrum Radiat. Transfer*, **96**, 139 (2005); www.elsevier.com/locate/jqsrt.
23. Fabelinskii I.L. *Usp. Fiz. Nauk*, **164**, 897 (1994) [*Phys. Usp.*, **37**, 821 (1994)].
24. Walrafen G.E., in *Water: A Comprehensive Treatise*. Ed. by F. Franks (New York: Plenum, 1972) Vol. 1; Walrafen G.E. *J. Phys. Chem.*, **94**, 2237 (1990); Castner E.W., Chang Y.J., Chu Y.C., Walrafen G.E., *ibid,* **102**, 653 (1995); Eisenberg D., Kauzmann W. *The Structure and Properties of Water* (Oxford: Clarendon Press, 2005).
25. Yamaguchi T., Matsuoka T., Koda S. *J. Chem. Phys.*, **120**, 7590 (2004).
26. Liou Y.-C., Tocilj A., Davies P.L., Jia Z. *Nature*, **406**, 322 (2000).
27. Pershin S.M., Adiks T.G., Luk'yanchenko V.A., Nigmatullin R.R., Potapov A.A. *Nelineinyi mir*, **7**, 79 (2009).